



**HAL**  
open science

## **Synthetic aperture time-reversal communications in shallow water: Experimental demonstration at sea**

W J Higley, Philippe Roux, W A Kuperman, W S Hodgkiss, H C Song, T Akal, Mark Stevenson

► **To cite this version:**

W J Higley, Philippe Roux, W A Kuperman, W S Hodgkiss, H C Song, et al.. Synthetic aperture time-reversal communications in shallow water: Experimental demonstration at sea. Journal of the Acoustical Society of America, 2005, 118, pp.2365 - 2372. 10.1121/1.2011147 . hal-04004283

**HAL Id: hal-04004283**

**<https://hal.science/hal-04004283>**

Submitted on 24 Feb 2023

**HAL** is a multi-disciplinary open access archive for the deposit and dissemination of scientific research documents, whether they are published or not. The documents may come from teaching and research institutions in France or abroad, or from public or private research centers.

L'archive ouverte pluridisciplinaire **HAL**, est destinée au dépôt et à la diffusion de documents scientifiques de niveau recherche, publiés ou non, émanant des établissements d'enseignement et de recherche français ou étrangers, des laboratoires publics ou privés.

See discussions, stats, and author profiles for this publication at: <https://www.researchgate.net/publication/228675386>

# Synthetic aperture time-reversal communications in shallow water: Experimental demonstration at sea

Article in *The Journal of the Acoustical Society of America* · October 2005

DOI: 10.1121/1.2011147

CITATIONS

32

READS

124

7 authors, including:



**Philippe Roux**

University Grenoble Alpes

494 PUBLICATIONS 12,931 CITATIONS

SEE PROFILE



**Tuncay Akal**

University of California, San Diego

135 PUBLICATIONS 3,315 CITATIONS

SEE PROFILE

Some of the authors of this publication are also working on these related projects:



Multivariate geophysical study of the Shallow structure of the Solfatara volcano - Campi Flegrei, Italy [View project](#)



Ocean Acoustic Tomography [View project](#)

# Synthetic aperture time-reversal communications in shallow water: Experimental demonstration at sea

W. J. Higley,<sup>a)</sup> Philippe Roux, W. A. Kuperman, W. S. Hodgkiss, H. C. Song, and T. Akal  
*Marine Physical Laboratory, Scripps Institution of Oceanography, University of California,  
San Diego, La Jolla, California 92093-0238*

Mark Stevenson

*NATO Undersea Research Centre, La Spezia, Italy*

(Received 15 April 2004; revised 6 July 2005; accepted 7 July 2005)

Time reversal has been shown as an effective way to focus in both time and space. The temporal focusing properties have been used extensively in underwater acoustics communications. Typical time-reversal communication experiments use vertical transducer arrays both to increase the signal-to-noise ratio and decrease the temporal sidelobes created in the time reversal process. Comparable temporal focusing is achieved using a horizontal array. In this paper, synthetic aperture time-reversal communications are accomplished, requiring only two transducers (one transmitter and one receiver). Deriving results from an at-sea experiment, this work confirms the viability of synthetic aperture time-reversal communications. © 2005 Acoustical Society of America. [DOI: 10.1121/1.2011147]

PACS number(s): 43.60.Tj, 43.60.Dh [DRD]

Pages: 2365–2372

## I. INTRODUCTION

Time reversal has been shown to be an effective way to combat the temporal spreading classically observed in a waveguide.<sup>1</sup> Indeed, after pulse transmission from a point source, if the wave forms recorded at a set of receivers are time-reversed and retransmitted simultaneously into the medium, the result is spatial focusing and temporal compression. Spatial focusing means that the time-reversed field is strong at the location of the original source and relatively weaker elsewhere in the medium. Specifically, spatial focusing implies that the ratio of the intensities between any point not at the focus and that of the focus is low. Temporal compression means that the time-reversed signal at the source has the same pulse width to the signal previously emitted by the source. Because time reversal refocuses the desired signal in time, it has been applied to underwater communications.<sup>2–4</sup>

Recent time-reversal communications experiments<sup>1–3</sup> have used a vertical array of transducers moored to the ocean bottom or hung over the side of a ship. Indeed, a vertical array provides spatial diversity that is turned into an advantage when time reversal is performed.<sup>5</sup> Proposed in this work is a communication system using a synthetic aperture<sup>6</sup> time-reversal array that would require only two transducers, a transmitter and a receiver, of which at least one is moving. The advantage of a synthetic aperture array is that it provides spatial diversity with the use of only one source. However, the drawback of a synthetic aperture array is that the wave forms are received at different times, as the transducer is only at one place at any given time. This makes synchronization an issue. Steps must be taken to coherently sum the

wave forms received on a synthetic aperture array. The motion of the transducer also induces a Doppler shift which may be different for each wave form, or even time varying. This must also be corrected before the received wave forms can be summed coherently.

Our proposed synthetic aperture communication system is based on the idea that a horizontal time-reversal array focuses well in the temporal domain.<sup>7</sup> Time reversal, as a simple and computationally inexpensive form of pulse compression, allows for a faster bit rate than systems without such pulse compression because intersymbol interference is mitigated. To affirm the feasibility of the proposed communication system to an oceanic environment, an experiment has been performed off the coast of Italy. The goal is to study, experimentally, the acoustical physics of a one-channel time-reversal communication system in a multipath environment. At this stage, no encoder/decoder (like turbo codes,<sup>8</sup> for example) or equalization<sup>9</sup> to potentially further reduce the error rate at the output of the communication system has been employed.

During the at-sea experiment, passive time reversal<sup>4</sup> rather than active time reversal is used. As long as the communications sequence sent from each synthetic aperture element is not too long, the Green's function used in passive time reversal can be viewed as time-invariant. This is in contrast to the concept that as the transducer moves from synthetic aperture element to element, the Green's functions vary.

The purpose of the experiment is to demonstrate the low bit error rates achievable at sea using a two-element system and passive synthetic aperture time reversal. Section II describes the experiment performed at sea and Sec. III details the processing done on the acquired data to extract the bit error rates. In Sec. IV, the possibility of using a few verti-

<sup>a)</sup>Author to whom correspondence should be addressed; electronic mail: bhigley@mpl.ucsd.edu

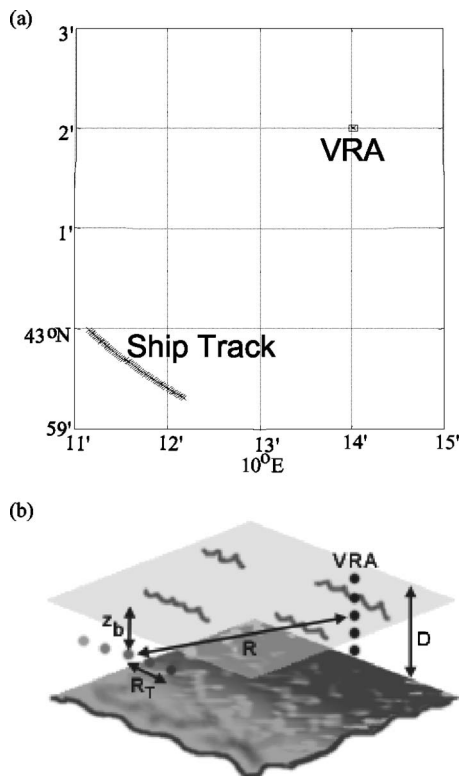


FIG. 1. (a) A vertical receiver array (VRA) moored off the coast of Italy received signals from a transducer towed by a moving vessel following the path shown. Each  $\times$  represents a position in the almost 2-km-long synthetic aperture array. It is of note that the synthetic aperture array is oriented in such a manner that the VRA is approximately broadside to the track. The average distance between the moving source and the VRA is 5.5 km. (b) The same setup from another angle, showing the depth of the water,  $D$ , the range of the synthetic aperture array,  $R$ , the depth of the array,  $z_b$ , and the distance along the track of a single element,  $R_T$ .

cally oriented hydrophones, which spans only a small portion of the water column, to further lower the bit error rates of the system is examined.

## II. EXPERIMENTAL DETAILS

A vertical receiver array (VRA) was moored off the coast of Italy, approximately 30 km north of the Island of Elba, where the mean depth,  $D$ , was approximately 120 m. In this environment, the sound speed was relatively constant, ranging from 1506 to 1508 m/s. From various geoacoustic experiments in the same area, the bottom properties were obtained through inversion yielding a sound speed of 1600 m/s and an attenuation of 0.3 dB/ $\lambda$ . This vertical array consisted of 32 elements each separated by 2 m, spanning from 30 to 92 m in the water column. A transducer was towed (at a 35-m depth) by a moving vessel at a speed of 2 knots on a track shown in Fig. 1. It is noticeable that the track is oriented such that the VRA is broadside to the synthetic aperture array (as viewed from above), as opposed to endfire. In a range-independent environment, the Green's function should not *a priori* vary over such a track path, thus limiting the gain in spatial diversity. However, at the frequency of 3 kHz, the wavelength (0.5 m) is very small compared to the propagation range ( $R \sim 5.5$  km) so that a minimal bathymetry change leads to a noticeable modification of

the Green's function. Also, the path is such that the VRA is not perfectly broadside to the track, and the small amount of range difference between elements may be enough to induce changes in the Green's function. A measure of the Green's functions change is discussed quantitatively in the following. The moving transducer transmitted a 1-ms pulse at 3 kHz, followed by a 10-s communication sequence coded using binary Amplitude Shift Keying (ASK), also at 3 kHz, consisting of 9800 bits with a bit length of 1 ms. The initial choice of an incoherent communication scheme [versus a coherent scheme like Binary Phase Shift Keying (BPSK)] was driven by its robustness to Doppler or synchronization issues.<sup>10</sup> The pulse and the communication sequence were separated by 200 ms so that they do not overlap after propagation through the dispersive channel. The purpose of the pulse is to probe the medium and to provide the Green's function that will be used to deconvolve the communication sequence.<sup>4</sup> The incident field was then received by all 32 channels on the vertical array, producing a matrix of Green's functions. In Sec. III, passive time-reversal is performed on one element of the vertical array only, whereas a 4-m vertical aperture made of three contiguous elements is used in Sec. IV. The pulse and communication sequence were transmitted every 30 s, each time producing a new Green's function matrix. During a 33-min-long track, 65 such matrices of Green's functions were acquired separated by a mean distance of 30 m. The synthetic aperture array thus consisted of up to 65 elements (though, typically no more than four at a time are examined in this paper) spanning just less than 2 km. The signal-to-noise ratio of the communication sequence varied between 25 and 30 dB over the ship track (see Fig. 5).

## III. DATA PROCESSING

### A. Decorrelation along the track

As can be seen in Fig. 1, the track of the moving transducer creates a synthetic aperture array, such that the VRA (as viewed from above) is oriented broadside to this array. Considering, for now, only one channel on the VRA (depth  $\sim 38$  m), the source depth, receiver depth, and range between the source and the receiver can all be considered approximately constant. To distinguish between different transmissions of the moving transducer, the variable,  $R_T$ , which is the distance along the track at the time of transmission, is introduced. Thus, the Green's function between a point on the track and the VRA can be written as  $G(t, R_T)$ . The fact that the synthetic aperture is oriented broadside to the VRA rather than endfire does not present a problem for the time-reversal process since the Green's function changes azimuthally, thereby providing the required spatial diversity. The change in Green's function is calculated as follows: The Green's functions are normalized to have unit power and autocorrelated. Each autocorrelated Green's function corresponds to the point-to-point time reversal between one VRA element and the moving source [see Eq. (1)]. Spatial diversity will be used efficiently if the time-reversal sidelobes cancel each other along the source track, i.e., the temporal sidelobes of the autocorrelated Green's function decorrelates as the source moves. The point-to-point time-reversal sidelobes<sup>1</sup>

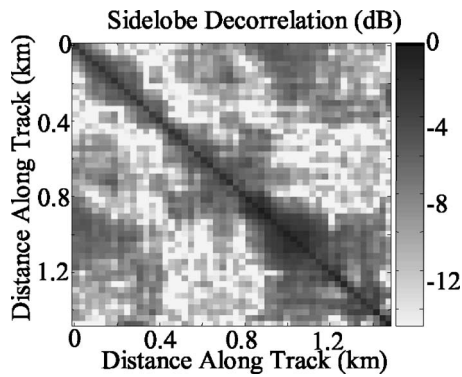


FIG. 2. Point-to-point time-reversal sidelobe decorrelation. These results are obtained by first normalizing the Green's functions at the distances along the track indicated on the axis, autocorrelating each of them, and then cross-correlating the resulting sidelobes. The results are a measure of how much the Green's function changes as a function of the distance along the track. The distance between Green's functions that results in a total decorrelation of the point-to-point time reversal sidelobes varies between 100 and 300 m.

decorrelation is shown in Fig. 2. It can be noticed that the Green's function changes enough to affect the sidelobes of the autocorrelation over a distance that varies between 100 and 300 m along the track.

The change in Green's functions along the track can be attributed to either the 30-m azimuthal or the 3-m radial distance (with respect to the VRA) between each source position. In the extreme case, where 300 m along the track is necessary to decorrelate the autocorrelation sidelobes, this corresponds to less than 300-m azimuthal distance and 30-m radial distance. There is an ambiguity as to which of these distances causes the decorrelation. However, this radial distance corresponds to 60 wavelengths, which is enough to cause a decorrelation of the field in the waveguide. In the other extreme case, where only 100 m is necessary to decorrelate the autocorrelation sidelobes, it is likely that a combination of azimuthal and radial distance changes is responsible for the decorrelation.

### B. Extracting bit error rates

After propagation through the channel, the received signals are not matched in frequency due to time-dependent Doppler shift. The Doppler shift may be either due to relative motion between the two transducers, or a mismatch between

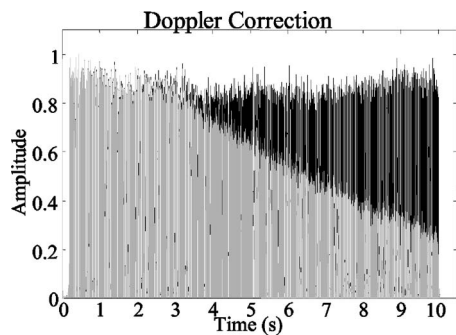


FIG. 3. The results of summing coherently the 65 received wave forms before Doppler correction (in gray) and after Doppler correction (in black). As time progresses, it is shown that the amplitude of the noncorrected sum decreases as the noncorrected signals do not add coherently at later times.

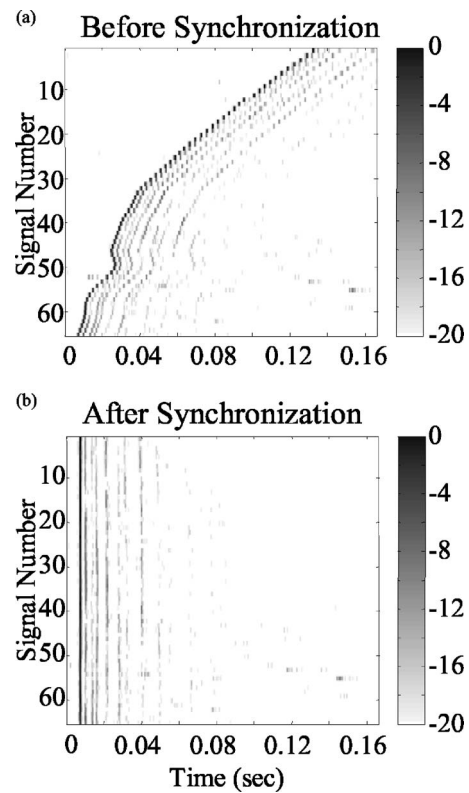


FIG. 4. The received wave forms before and after synchronization. Synchronization is an issue as time-reversal cannot be performed simultaneously from the synthetic aperture array. The signals must be accurately synchronized before time-reversal so they may be summed coherently. Shown are the received wave forms in dB, normalized to the maximum.

the sampling frequencies of the transducers. Also, as the signals are not received simultaneously, they are not synchronized in time. Both of these effects must be compensated before the signals can be added coherently.

To correct for the Doppler shift, a Fast Fourier Transform (FFT) is taken of the zero-padded communications sequence. As the Green's functions of this data set have a strong ballistic path and the communications are encoded with ASK, in the absence of Doppler shift, one would expect a strong peak at 3 kHz, the carrier frequency. Due to Doppler effects, this peak is shifted a small amount, ranging from 0.4 to 0.9 Hz. If the motion of the transducer were endfire, one would expect the Doppler shift to be greater. The signal is then dilated or compressed in time so that the value of the peak is shifted back to 3 kHz. Figure 3 shows the coherent sum over the synthetic aperture of all received time-domain signals (after synchronization and time reversal described in the following) with no Doppler correction in gray, and with Doppler correction in black. It is seen that the two sums are similar in amplitude at the beginning, but that as time progresses, the amplitude of the noncorrected sum decreases. This is due to the fact that the noncorrected signals do not add coherently at later times.

Once the signal has been Doppler corrected, the next step is to synchronize the signals in time. In order to do that, the signals with the highest signal-to-noise ratio is used as a reference. As mentioned earlier, the received signal consists of two parts, the dispersed pulse, which has become the

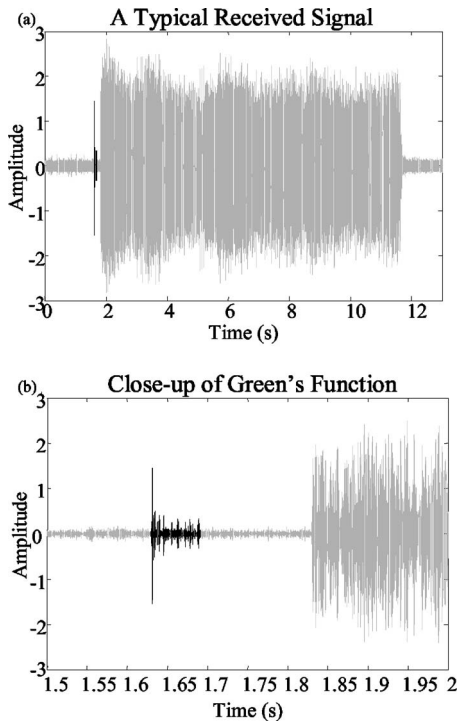


FIG. 5. (a) A typical received signal consisting of an initial pulse and a 10-s communication sequence, after both have propagated through the medium. The selected Green's function is shown in black. (b) The same signal, zoomed in to show the detail of the Green's function, which has spread from an original 1-ms pulse, to a 70-ms-long dispersed signal. Signal-to-noise ratio is about 25 dB.

Green's function, and the dispersed communication sequence. In order to synchronize the wave forms, one may focus on the Green's function. Knowing the time between the beginning of the Green's function and the communication sequence (200 ms), the synchronization of the Green's functions along the track yields the synchronization of all the communication sequences. Figure 4 shows the 65 Green's functions received before and after synchronization. For each of the 65 received wave forms the following steps are taken. The Green's functions are time-gated to select the first arrival of the impulse response. The first arrivals are then synchronized along the aperture using cross correlation. After synchronization of the first arrival a larger time window, ap-

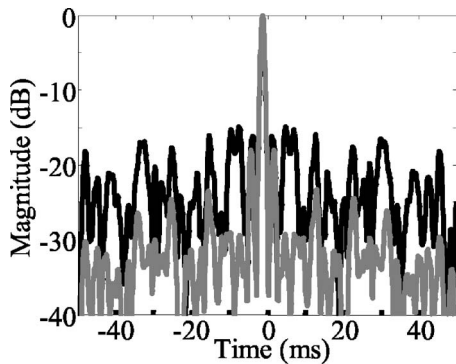


FIG. 6. The Q-function (Ref. 10) resulting from a single element is shown in black, and from the coherent summation of five widely spaced elements is shown in gray. It can be seen that the summation results in lower sidelobe levels, which produce lower bit error rates.

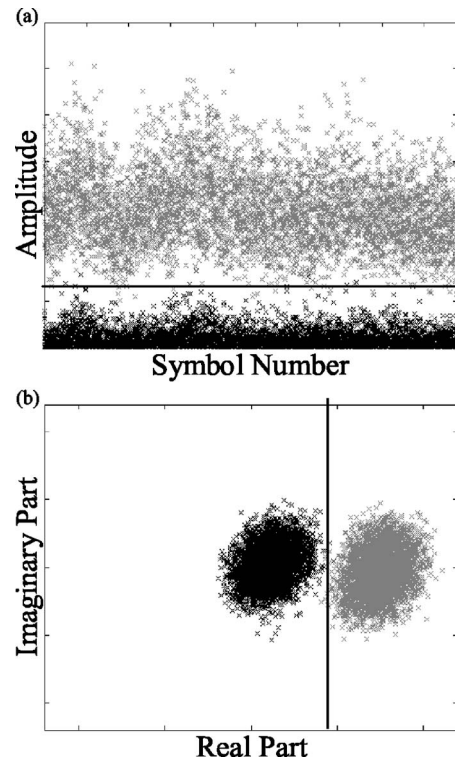


FIG. 7. (a) The results of incoherently decoding a signal composed of the sum of three widely spaced synthetic aperture elements, that is synthetic aperture elements that have decorrelated Q-function sidelobes. Binary 0s are shown in black, binary 1s are shown in gray, and a threshold is indicated by a dark line. The number of errors in the case shown was 31, giving a bit error rate of 0.32%. (b) The results of decoding the same signal coherently. Again, binary 0s are shown in black, binary 1s are shown in gray, and a threshold is indicated by a dark line. The number of errors in this case, decoded coherently was 7, giving a bit error rate of 0.071%.

proximately 70 ms, is taken and designated the Green's function. Figure 5 shows a typical signal received on the VRA, with the selected Green's function darkened. In the case of a set of Green's functions lacking a dominant first arrival, the method of synchronization would have to be modified.<sup>6</sup> For example, a particularly strong and stable path of the Green's function could be chosen in place of the first arrival. In the case of low signal-to-noise ratios, one could consider that the only thing in common between any two received wave forms is the communication sequence,  $m(t)$  [see Eq. (1)]. Cross correlation between received wave forms will exhibit a peak when the embedded sequence in each wave form overlaps. The time at which these peaks occur correspond to the relative delay in each received signal. By removing this delay, the signals are synchronized.

After synchronization, each Green's function is extracted, time reversed, and convolved with the communication sequence to cancel the multipath propagation as classically done in passive time-reversal. The result of these convolutions is 65 wave forms that can be summed coherently to produce the message estimate, written as

$$\hat{m}(t) = m(t) * \sum_j [G(-t, R_{Tj}) * G(t, R_{Tj})], \quad (1)$$

where  $m(t)$  is the coded communication sequence. The summation part of the equation has been referred to as the

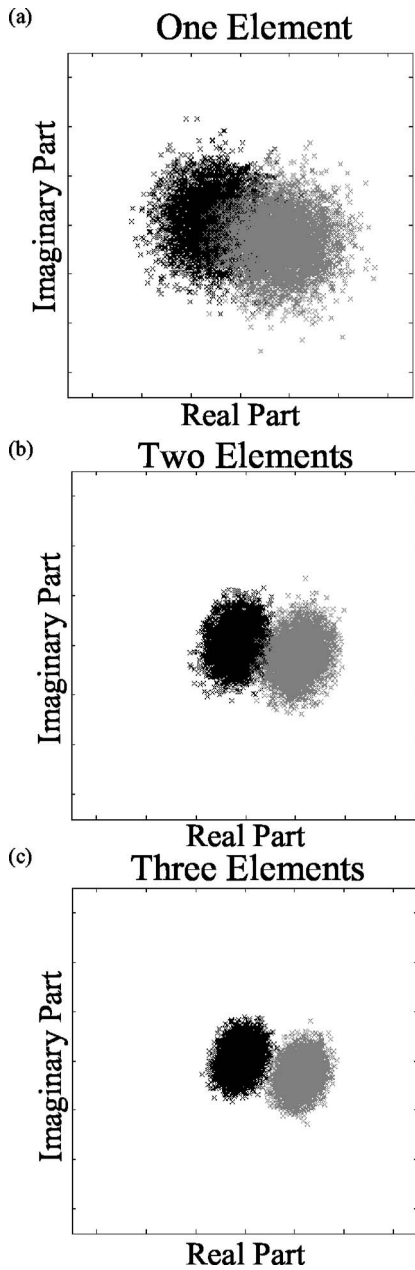


FIG. 8. The evolution of the in-phase/quadrature plot as more synthetic elements are summed together before decoding. The elements added are widely spaced. Binary 0s are in black and binary 1s are in gray.

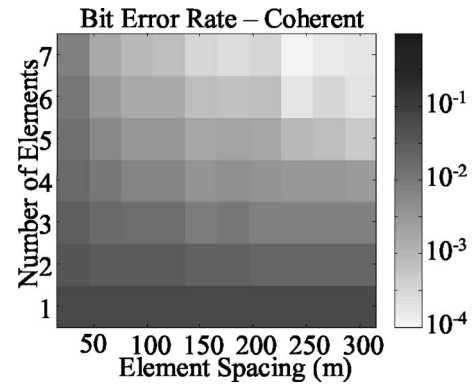


FIG. 9. Bit error rate found from 9800 bits, each with a bit length of 1 ms, as a function of the number of transducer positions (or synthetic array elements) for various values of element spacing,  $\delta R_T$ .

Q-function.<sup>10</sup> A typical Q-function for one element (which is the point-to-point time-reversal described in Sec. III A) and for five elements is shown in Fig. 6. As expected, the time-reversal sidelobes are reduced as more elements are added coherently, suggesting that better communication can be achieved with a time reversal synthetic aperture.

Although the modulation used (ASK) is an incoherent modulation, it can be demodulated either incoherently or coherently. In either case, the message estimate is base-banded by multiplication with a sinusoid at the carrier frequency and filtered. The resulting wave form is then resampled at the symbol rate producing  $N$  complex numbers, where  $N$  is the number of symbols. To demodulate incoherently, the absolute value of each of these numbers is compared to a threshold to determine whether the bit is a binary 1 or a binary 0. The threshold is chosen as half the mean of the  $N$  positive numbers. Figure 7(a) shows the resulting values from incoherent modulation before the hard decision is made. The figure was made using only three widely spaced synthetic aperture elements with decorrelated Q-function sidelobes. In Fig. 7(a), binary 0s are shown in black and binary 1s are shown in gray. The threshold is shown by a dark line. To demodulate coherently, the real part of each of the  $N$  complex numbers is compared to a threshold to determine whether the bit is a binary 1 or a binary 0. The threshold is chosen as the mean of the real part of the  $N$  complex numbers. Figure 7(b) shows the resulting values from the coherent modulation before the hard decision is made. This figure was made using the same three widely spaced synthetic ap-

TABLE I. Selected values of the bit error rate found from 9800 bits, each with a bit length of 1 ms, as a function of the number of transducer positions (or synthetic array elements) for various values of element spacing,  $\delta R_T$ .

$\delta R_T$ (m)	Data rate in bits per second (number of elements in the synthetic aperture)						
	1000 (1)	500 (2)	333 (3)	250 (4)	200 (5)	167 (6)	143 (7)
30	$6.9E-2$	$4.2E-2$	$2.8E-2$	$2.0E-2$	$1.5E-2$	$1.0E-2$	$7.5E-3$
60	...	$3.6E-2$	$2.0E-2$	$1.1E-2$	$6.1E-3$	$3.1E-3$	$1.6E-3$
150	...	$2.6E-2$	$9.5E-3$	$4.1E-3$	$1.9E-3$	$8.5E-4$	$3.2E-4$
300	...	$2.1E-2$	$7.6E-3$	$2.9E-3$	$5.3E-4$	$2.3E-4$	$2.0E-4$

(a) XXXXOOOO++++  
 (b) X X X X O O O O + + + +  
 (c) XO+ XO+ XO+ XO+

FIG. 10. Schematic of a synthetic aperture time reversal communication system. For the sake of simplicity, the communication sequences are represented by the symbols  $\times$ ,  $\circ$ , and  $+$ . (a) Multiple sequences transmitted as quickly as allowed by the equipment. (b) The same sequences, with the spacing between transmissions increased in order to increase the length of the synthetic aperture endfire aperture. This creates a better focus and decreases the bit error rate. (c) By interleaving sequences, one may achieve the same bit error rate as in step b, but maintains the same data rate as in step a.

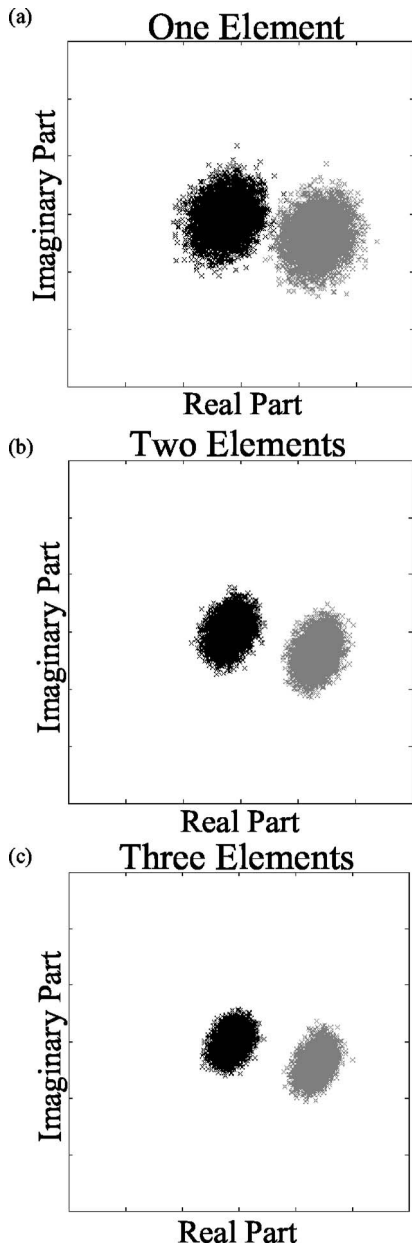


FIG. 11. The evolution of the in-phase/quadrature plot as more vertical elements are summed together before decoding. Before summation over the vertical elements, a horizontal synthetic aperture of three widely spaced elements is used.

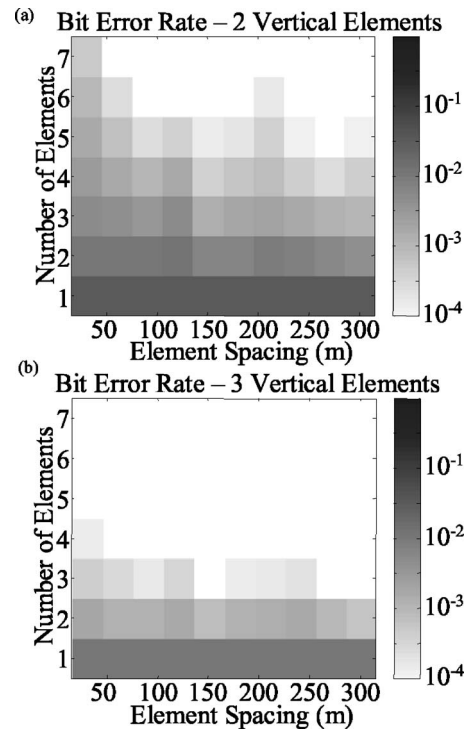


FIG. 12. Bit error rate found from 9800 bits, each with a bit length of 1 ms, as a function of the number of synthetic array elements, element spacing,  $\delta R_T$ , and number of vertical array elements. The bit error rates using only one vertical element can be found in Fig. 9.

erture elements. Again, binary 0s are shown in black, binary 1s are shown in gray, and threshold is shown by a dark line. The comparison between the estimate sequence and the sequence sent produces a bit error rate. From Fig. 7, it can be deduced that coherent demodulation is not only possible, but gives lower bit error rates than the incoherent demodulation. From this, one may anticipate that it is possible to use synthetic aperture time reversal with more complicated, coherent modulation techniques such as BPSK or Quaternary Phase Shift Keying (QPSK). As coherent demodulation gives lower bit error rates, the rest of the paper presents results for coherent modulation. Lower bit error rates are expected as more synthetic aperture elements are added together, which is seen in Fig. 8. This figure shows the evolution of the in-phase/quadrature plot as synthetic aperture elements are summed. As seen in Fig. 8, the result of using more synthetic aperture elements are tighter clouds of points and ultimately, lower bit error rates.

### C. Results

We present the bit error rates as a function of two parameters of the synthetic aperture array: the number of elements used in summation and the element spacing. Despite the orientation of the track, such that the VRA is broadside to it, it is shown that the Q-function sidelobes decorrelate as the distance along the track increases, thus element spacing plays an important role in determining bit error rates. Results are shown as a grayscale plot in Fig. 9. The bit error rate decreases as the number of elements is increased and also decreases as the element spacing is increased. However, by increasing the number of elements used, as this is a synthetic

TABLE II. Selected values of the bit error rate found from 9800 bits, each with a bit length of 1 ms, summed over three vertical elements, as a function of the number of transducer positions (or synthetic array elements) for various values of element spacing,  $\delta R_T$ .

$\delta R_T$ (m)	Data rate in bits per second (number of elements in the synthetic aperture)						
	1000 (1)	500 (2)	333 (3)	250 (4)	200 (5)	167 (6)	143 (7)
30	$1.0E-2$	$1.9E-3$	$4.4E-4$	$1.4E-4$	$7.3E-5$	$2.5E-5$	$1.4E-5$
60	...	$1.3E-3$	$2.8E-4$	$5.3E-5$	$1.8E-5$	$3.7E-6$	0
150	...	$7.6E-4$	$7.1E-5$	$4.1E-6$	$2.2E-6$	0	0
300	...	$6.1E-4$	$7.7E-5$	$2.3E-5$	$4.1E-6$	0	0

aperture, the effective data rate is diminished. Using only one element in the system, corresponding to a data rate of 1000 bps, yields a bit error rate of 7%. By using two elements spaced 300 m apart, corresponding to a data rate of 500 bps, the bit error rate is dramatically lowered to 2.1%. An increase to three elements with a mean spacing of 300 m, corresponding to a data rate of 333 bps, yields a bit error rate below 1%.

#### D. Interleaving communication sequences

If one were to transmit as quickly as allowed by the equipment, the element spacing,  $\delta R_T$ , would be small, requiring a large number of transducer positions to achieve a low bit error rate. For instance, in Table I, it is shown that it takes seven elements to achieve a bit error rate of 0.75% when the element spacing is only 30 m, but when the element spacing is 300 m, the same bit error rate is achieved with only three elements. The spacing of 300 m is chosen from the decorrelation of the Q-function sidelobes shown in Fig. 2. If one were to simply increase the aperture by increasing the element spacing,  $\delta R_T$ , there would be times when the transducers were unused since it is necessary to wait for one of the transducers to move and the aperture to further increase. In this spare time between transmissions of the first communication sequence, other sequences can be sent. By interleaving communication sequences, the data rate is the same as the fastest allowed by the equipment, but the bit error rate will be significantly lower. Figure 10 demonstrates this concept graphically.

#### IV. VERTICAL SUMMATION

The experiment at sea was done using a vertical array consisting of 32 elements, only one of which has been used so far in decoding the data. By using up to three contiguous elements, one may examine the decrease in bit error rate that would occur if one were to use a 4-m-long vertical array (centered at 38 m) that spanned only a small portion of the 120-m-deep water column. Such an array would still be relatively cheap, one of the primary advantages of the proposed system. The in-phase/quadrature plots resulting from the summation over a small number of vertically oriented elements are shown in Fig. 11. The summation is done vertically after the horizontal summation had been done over three widely spaced synthetic aperture elements. The bit error rates using a small number of vertically oriented elements

are presented in Fig. 12. The addition of a few vertical elements dramatically lowers the bit error rates of the system. For example, with a synthetic aperture of four elements, a vertical line array of three elements yields 12 wave forms that can be coherently summed. The results demonstrate that with a vertical line array of three elements, at three locations forming a synthetic horizontal line array, bit error rates lower than  $10^{-5}$  can be achieved with a 1-ms bit length (Table II).

#### V. CONCLUSION

This paper serves to confirm the feasibility of an inexpensive communication system using a synthetic aperture time reversal array at sea. The main benefit of this system is that it requires only two transducers (one transmitter and one receiver), significantly decreasing the technological cost compared to typical time reversal communication schemes. The disadvantage of this system is that the repeated transmission of the communication sequence tends to lower to data rate. As in many communication systems, a tradeoff must be made between the data rate and the desired bit error rate. It is also shown that the addition of a few transducers oriented vertically in addition to the horizontal aperture significantly decreases the bit error rate without a significant increase in cost or complexity of the system. Finally, it is reiterated that this study is limited to how synthetic aperture time reversal can utilize shallow water propagation complexity; additional communication algorithms can always be appended to increase performance.

<sup>1</sup>W. A. Kuperman, W. S. Hodgkiss, H. C. Song, T. Akal, C. Ferla, and D. Jackson, "Phase conjugation in the ocean: Experimental demonstration of an acoustic time-reversal mirror," *J. Acoust. Soc. Am.* **98**, 25–40 (1998).

<sup>2</sup>G. F. Edelmann, T. Akal, W. S. Hodgkiss, S. Kim, W. A. Kuperman, and H. C. Song, "An initial demonstration of underwater acoustic communication using time reversal," *IEEE J. Ocean. Eng.* **27**, 602–609 (2002).

<sup>3</sup>K. B. Smith, A. A. M. Abrantes, and A. Larraza, "Examination of time-reversal acoustics in shallow water and applications to noncoherent underwater acoustic communications," *J. Acoust. Soc. Am.* **113**, 3095–3110 (2003).

<sup>4</sup>D. Rouseff, D. R. Jackson, W. L. J. Fox, C. D. Joes, J. A. Ritcey, and D. R. Dowling, "Underwater acoustic communication by passive phase conjugation: Theory and experimental results," *IEEE J. Ocean. Eng.* **26**, 821–831 (2001).

<sup>5</sup>P. Roux and M. Fink, "Time reversal in a waveguide: Study of the temporal and spatial focusing," *J. Acoust. Soc. Am.* **107**, 2418–2429 (2000).

<sup>6</sup>S. Stergiopolous, "Implementation of adaptive and synthetic-aperture processing schemes in integrated active-passive sonar systems," *Proc. IEEE* **86**, 358–398 (1998).

<sup>7</sup>M. R. Dungan and D. R. Dowling, "Orientation effects on linear time

reversing array retrofocusing in shallow water," *J. Acoust. Soc. Am.* **112**, 1842–1852 (2002).

<sup>8</sup>C. Berrou and A. Glavieux, "Near optimum error correcting coding and decoding: turbo-codes," *IEEE Trans. Commun.* **44**, 1261–1271 (1996).

<sup>9</sup>G. F. Edelmann, S. Kim, W. S. Hodgkiss, W. A. Kuperman, H. C. Song, and T. Akal, "Combining and comparing time reversal processing and

adaptive channel equalization for communications sequences," *J. Acoust. Soc. Am.* **112**, 2447 (2002).

<sup>10</sup>T. C. Yang, "Temporal resolution of time-reversal and passive-phase conjugation for underwater acoustic communications," *IEEE J. Ocean. Eng.* **28**, 229–245 (2003).